Influence of Wilbraham-Gibbs Phenomenon on Digital Stochastic Measurement of EEG Signal Over an Interval

P. Sovilj[1], M. Milovanović[2], D. Pejić[1], M. Urekar[1], Z. Mitrović[1]

[1] Department of Power, Electronics and Communication Engineering, Faculty of Technical Sciences, University of Novi Sad, Trg Dositeja Obradovića, 6, 21000, Novi Sad, Serbia, platon@uns.ac.rs
[2] Military Health Academy, Crnotravska, 17, 11000, Belgrade, Serbia, vma@mod.gov.rs

Measurement methods, based on the approach named Digital Stochastic Measurement, have been introduced, and several prototype and small-series commercial instruments have been developed based on these methods. These methods have been mostly investigated for various types of stationary signals, but also for non-stationary signals. This paper presents, analyzes and discusses digital stochastic measurement of electroencephalography (EEG) signal in the time domain, emphasizing the problem of influence of the Wilbraham-Gibbs phenomenon. The increase of measurement error, related to the Wilbraham-Gibbs phenomenon, is found. If the EEG signal is measured and measurement interval is 20 ms wide, the average maximal error relative to the range of input signal is 16.84 %. If the measurement interval is extended to 2s, the average maximal error relative to the range of input signal is significantly lowered – down to 1.37 %. Absolute errors are compared with the error limit recommended by Organisation Internationale de Métrologie Légale (OIML) and with the quantization steps of the advanced EEG instruments with 24-bit A/D conversion.

Keywords: Biomedical measurement, EEG, stochastic measurement, Wilbraham-Gibbs phenomenon.

1. INTRODUCTION

ELECTROENCEPHALOGRAPHIC (EEG) measurements are commonly used in medical and research areas [1]. The EEG signals are small electrical potentials (generally less than 300 µV) produced by the brain [2-3]. The frequencies of these brain produced signals can range from 0.5 to 100 Hz, and their characteristics are highly dependent on the degree of activity of the cerebral cortex [4]. From a hardware standpoint [3], electroencephalograms have traditionally been the most difficult electrogram measurements to acquire.

Typically, an EEG measurement system is comprised of electrodes and cables, a conditioning module, a digitizing module, and a module for performing data processing, recording and presenting. The electrodes are usually Ag/AgCl electrodes contained within a net or a hat placed on the scalp of a patient; the net or the hat would then connect to the conditioning module using a cable, subjecting the microvolt level EEG signal to the ambient noise, being many times greater than the signal itself. To amplify such low level EEG signal, the conditioning module incorporates amplifying circuits with a high gain (5000-20000 times), but also Driven Right Leg (DRL) circuit [5] and high-order analog filters with a sharp roll-off, to ensure that only the desired signal is detected [6-7]. EEG data processing has an increasingly important role, because of the importance of many spectral measures and nonlinear measures [8-12]. For example, such measures can be useful for detection of different brain states during subject training with audio-visual stimulation [8, 9], or can be suitable for the detection of different sleep stages [11, 12].

Generally speaking, the advanced measurement instrumentation is based on digitizing hardware components, having measuring signals usually conditioned, while the time-continuous conditioned signals are sampled and converted into discrete digital variables. During the A/D conversion process, the accuracy and speed are opposing requirements, so that accurate measurements of low-level, noisy and distorted signals have been a challenging problem in the theory and practice of measurement science and technology. A possibility for reliable operation of instruments with inherent random error has been researched since 1956 [13], and inherent property of such an approach is a very simple hardware structure. Therefore, such instruments can operate very fast and can be easily miniaturized into integrated circuits. It has been shown that adding a random uniform dither to an A/D converter input can decouple measurement error from the input signal [14-15]. This dither also suppresses the measurement error due to both coarse A/D conversion and the external additive noise in the input signal.

Following this measurement strategy, several specific methods have been developed for measuring average DC inputs, AC inputs and/or distorted AC inputs. Several prototype and small-series commercial instruments have been realized and calibrated, and their measurement uncertainty can be extremely low [16-19]. The approach of those methods was named Digital Stochastic Measurement (DSM) and these instruments were named Digital Stochastic Instruments.

For example, a prototype instrument, reported in [18] can perform the harmonic analyses for the DC component and up to 49 harmonics (both cosine and sine components) in each of the seven different input channels. Its operation is based on stochastic A/D conversion and accumulation, with a hardware structure designed for the harmonic measurement. The method and the predicted uncertainty for 50 harmonics are validated in [18] by simulation and experiments using the sampling frequency of 250 kHz per channel. In [19] a DSM method is investigated for various types of stationary signal. The results demonstrate the ability

of this method to be applied for measurement of harmonics of any stationary signal. Improvement of this method is presented in [20], for the cases when fundamental frequency drifts from its nominal value as is the case with real power grid signals.

If the EEG measurement system in Fig.1. is implemented correctly, the conditioning of EEG signal is generally satisfying for accurate measurements. However, if the EEG system is exposed to high-level ambient noise (e.g., when EEG measurements are combined with magnetic resonance imaging (MRI) where imaging artifacts appear and signal-to-noise ratio (SNR) can be extremely low), then this conditioning techniques are not satisfying. In these cases, it is necessary to apply some digital data processing for extracting the EEG signal [21-24].

Papers [25, 26] are the result of researching alternative solutions for such situations of a high-level ambient noise presence, and they describe the implementation of the DSM approach in measurement of non-stationary signal harmonics with varying measurement time. Measurement uncertainty in [25] is calculated by the developed theory while the EEG signal is selected as an example of real non-stationary signal. Digital stochastic measurement of EEG signal harmonics is tested by simulations and by experiments in [25, 26]. Tests are done both without adding noise and with adding noise (SNR varies from 10dB to -10 dB). The results of simulations and experiments are compared with theory calculations, so that comparison confirms the theory. The presented method provides decrease of the measurement uncertainty even at low SNR values, by increasing the A/D converter's sampling rate. This enables designers of measurement systems to achieve higher measurement accuracy in the high-level ambient noise presence, by choosing fast A/D converters with low resolution.

Following the previous research [25], this paper investigates the problem of influence of the Wilbraham-Gibbs phenomenon [27-29] on digital stochastic measurement of EEG signal in the time domain. The increase of measurement error is recognized as the consequence of the Wilbraham-Gibbs phenomenon. This measurement error is analyzed and discussed for sometypical waveforms and for the EEG signal. Finally, design recommendation for EEG stochastic instrument is proposed, regarding minimization of this error.

2. METHOD AND THE WILBRAHAM-GIBBS PHENOMENON

Concept of typical digital measurement of EEG signal is presented in Fig.1., while digital stochastic measurement of EEG signal over an interval is shown in Fig.2.

In the well-known digital measurement approach (Fig.1.), each digital value y_i ($i = 1, 2, ...$) is actually a result of digitizing an appropriate analog sample from the input (x_{ai}). These digitized samples y_i are obtained sample by sample, and frequency components are calculated after obtaining the required number of samples. Calculation of the frequency components is based on the Fourier transform. If the Fourier transform is applied to an input signal $x(t)$, by window function of a width equaling the measurement interval [0, T], then $x(t)$ can be presented as a trigonometric polynomial:

$$x(t) = \frac{a_0}{2} + \sum_{n=1}^{M} a_n \cos n\omega_0 t + \sum_{n=1}^{M} b_n \sin n\omega_0 t , \ 0 < t < T \qquad (1)$$

where a_i and b_i are Fourier coefficients, $\omega_0 = 2\pi/T$ and M is the order of trigonometric polynomial [30].
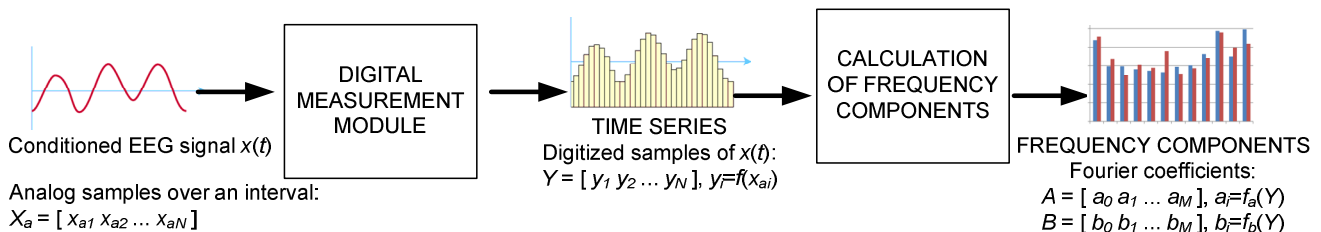

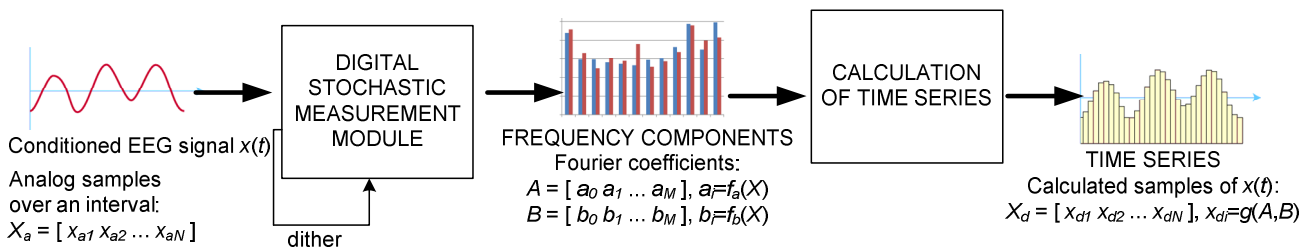Fig.1. Typical digital measurement of EEG signal.

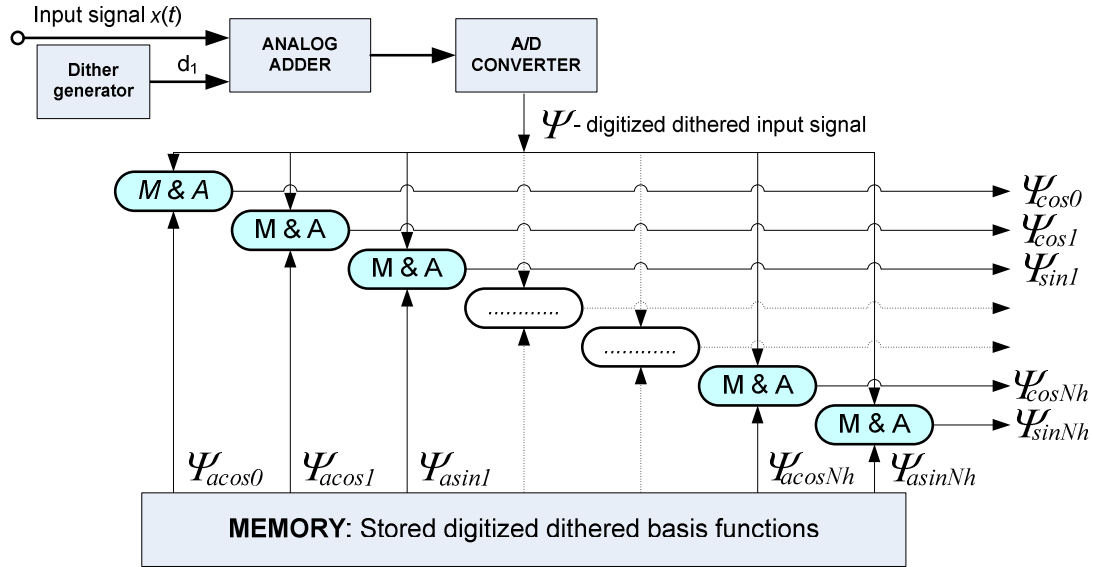Fig.2. Digital stochastic measurement of EEG signal over an interval.

Fig.3. Block-diagram of DSM module.

However, opposite to the well-known digital measurement approach, in the DSM approach, frequency components are measured first and appropriate time series is calculated afterwards. Each Fourier coefficient is obtained (by the DSM module) from all analog samples $X = [x_{a1}, x_{a2}, ..., x_{aN}]$ over the measurement interval $[0, T]$. Hence, this measurement is not based on "sample by sample" approach, but it is an interval-based approach. When the measurement interval is finished, the time series can be calculated by applying (1) at each time instant over the interval, or by using Inverse Fast Fourier Transform (which is a faster method). Therefore, results of digital stochastic measurement of the input signal over the measurement interval $[0, T]$ are completed as: a) the set of frequency components and b) the calculated time series, respectively (Fig.2.).

If it is required to measure the signal over the longer measurement interval $[0, Tm]$, where $Tm = m \cdot T$, the required measurement interval can be divided into smaller subintervals $[0, T]$, $[T, 2T]$, ... , $[(m-1)T, mT]$ and the method can be applied over each subinterval, respectively. Finally, when the interval $[0, Tm]$ is finished, the input signal is determined in the time domain over the whole measurement interval, by joining all the time series data in the appropriate order.

Fig.3. presents the block-diagram of DSM module as follows: $x(t)$ is the input signal, d_1 is the dither signal, Ψ is the digitized dithered input signal, the memory which provides digitized dithered basis functions, and M&A element which represents digital multiplier and digital accumulator (Ψ_{cosi} and Ψ_{sini} are the values accumulated in the accumulators). Dither d_1 satisfies following conditions (limitation of the dither amplitude and definition of probability density function of the dither):

$$0 \leq |d_i| \leq \frac{\Delta_1}{2} \qquad (2)$$

$$p(d_i) = \frac{1}{\Delta_1} \qquad (3)$$

Fourier coefficients of the input signal can be calculated as [18]:

$$a_i = \frac{2\overline{\Psi}_{\cos i}}{B}, \ b_i = \frac{2\overline{\Psi}_{\sin i}}{B} \qquad (4)$$

where B is the amplitude of basis functions. Also, appropriate standard measurement uncertainty is limited by [25]:

$$u(a_i) = u(b_i) \leq \sqrt{2} \cdot (\sigma_n + \Delta_1 / 2) / \sqrt{N} \qquad (5)$$

where σ_n^2 is a variance of any noise superimposed to the measured EEG signal, while N is the number of samples over the measurement interval. Complete details on derivation of measurement uncertainty for a_i and b_i can be found in [18, 25].

Each sine and cosine component requires a digital multiplier and a digital accumulator. Therefore, if the system measures the DC component and N_h harmonics, the DSM module will require $2N_h+1$ multipliers and $2N_h+1$ accumulators. At the first sight, according to these numbers, block diagram in Fig.3. seems to require very complex hardware implementation. However, its hardware implementation can be very simple by using the Field-programmable gate array (FPGA) device.

When the Fourier sums are calculated for a function, the Wilbraham-Gibbs phenomenon [26-27] includes both the fact that Fourier sums overshoot at the function jump discontinuity, and that this overshoot does not decrease as the fundamental frequency increases [28]. According to the Wilbraham-Gibbs phenomenon, at any jump point of a piecewise continuously differentiable function with a jump of a, the nth partial Fourier series will (for very large n)

overshoot this jump by approximately $a \cdot (0.089490...)$ at one end and undershoot it by the same amount at the other end [28]. Hence, the jump in the partial Fourier series will be about 18 % larger than the jump in the original function. Also, at the location of the discontinuity itself, the partial Fourier series will converge to the midpoint of the jump [28].

Because of the Wilbraham-Gibbs phenomenon, if the DSM approach is applied and if there is a discontinuity between the first and the last analog sample over a measurement interval, the measurement error would be increased. The next chapter analyzes and discusses the appearance and fluctuation of this measurement error.

3. RESULTS AND DISCUSSION

Simulation and experimental research of the method were conducted in two phases. In the first phase, the method was simulated with four typical waveforms as input signals: square wave, triangle wave, sawtooth wave and sine wave. In the second phase, the method was simulated and experimentally applied to various sequences of the EEG signal for two different measurement intervals – 20 ms and 2 s.

A. Measurement of typical waveforms.

Parameters of the measurement system are presented in Table 1. Simulations are performed with simulation model implemented in Matlab and VisualC and verified in previous extensive experimental verifications [16-19, 25]. Measurement interval of 20 ms is chosen, because the developed instrument supports this interval (fundamental frequency of 50 Hz).

In Fig.4. the input signal and result of measurement are compared, when sine wave is provided as the input signal. The amplitude of sine wave is 1 V and the frequency is 50 Hz. The maximal error is 0.06 V, so that the maximal error relative to the range of input signal is 2.93 %.

Table 1. Properties of measurement system with 20 ms measurement interval.

Property	Values
A/D conversion (Fig. 3)	Resolution: m_1=6 bits Input range: ±R and R=2.5 V Sampling frequency: f_{ADC} = 15625 Hz
Dither d_1	$0 \le |d_i| \le 39.7 mV$
Measurement interval	$[0,T]$ and T = 20 ms
Fundamental frequency	$f_0 = 1/T$ = 50 Hz
Number of samples per measurement interval	N = 312
Digital dithered base functions	Stored in memory in 64-bit floating point resolution but passed to the multiplier in 8-bit resolution, thus faithfully simulating an A/D converter with properties: Resolution: m_2 = 8 bits Range: ±R and R=2.5 V Sampling frequency: f_{ADC} = 15625 Hz
Number of measured Fourier coefficients	DC component + 49 sine coefficients + 49 cosine coefficients

In order to produce discontinuity between input values at the end and the start of the measurement interval, the frequency of the input sine wave is changed to 40 Hz. Comparison of the modified input sine wave and result of measurement is presented in Fig.5. The maximal error is 0.40 V, while the maximal error relative to the range of input signal is 20.09 %. In Fig.5. we can see that the measurement error is almost the same as for the 50 Hz sine wave, except at the edges of the measurement interval (where the error is increased).
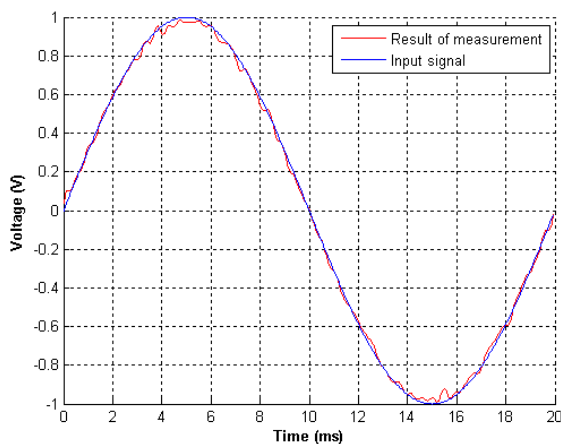

Fig.4. Comparison of input signal and result of measurement, when sine wave is provided as the input signal. Amplitude of the sine wave is 1 V, and frequency is 50 Hz..
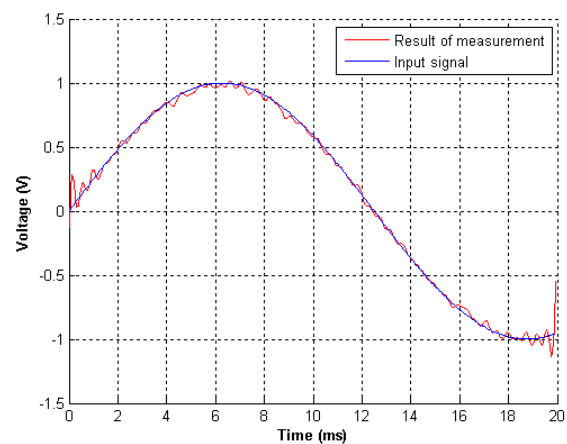

Fig.5. Comparison of input signal and result of measurement, when sine wave is provided as the input signal. Amplitude of the sine wave is 1V, and frequency is 40 Hz.

This relatively high error appears at the edges of the measurement interval (at the places of the produced discontinuity), so that it can be explained by the Wilbraham-Gibbs phenomenon. There is no discontinuity when the 50 Hz input sine wave is provided; hence the error is not abruptly increased at the edges of the measurement interval.

Comparison of the input signal with the result of measurement, when square wave is provided at the input, is presented in Fig.6. (the amplitude of square wave is 1V while the frequency is 50 Hz). The maximal error is 0.70 V, while the maximal error relative to the range of the input signal is 34.93 %. It can be noticed that the measurement error is increased at the middle and at the edges of the measurement interval. Again, these increased errors, at the places of the input signal discontinuities, can be explained by the Wilbraham-Gibbs phenomenon.
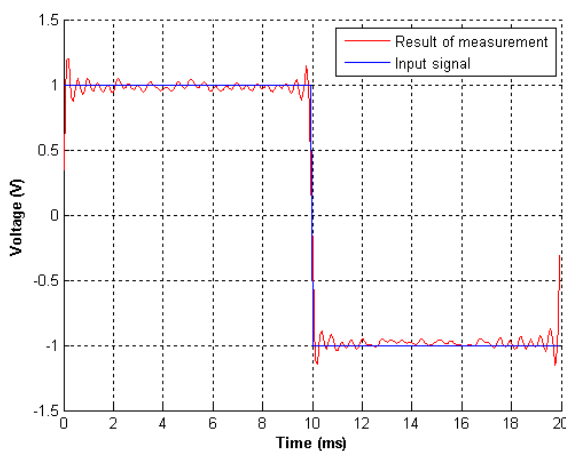

Fig.6. Comparison of input signal and result of measurement, when square wave is provided as the input signal. Amplitude of the square wave is 1V, and frequency is 50 Hz.

Also, simulation of measurement is done for triangle and sawtooth waves at the input. For triangle wave of 1V amplitude and 50 Hz frequency, the maximal error is 0.06 V and the maximal error relative to the range of input signal is 2.93 %. If the frequency of the triangle wave is changed to 40 Hz, the maximal error is increased to 0.46 V, so that the maximal error relative to the range of the signal is 23.15 %. As in the cases with sine waves, relatively high error appears for 40 Hz wave, because of the signal discontinuity, but the error is significantly lower for 50 Hz triangle wave. For sawtooth wave at the input, when amplitude is 1 V and frequency is 50 Hz, the maximal error is 0.72 V and the maximal error relative to the range of the input signal is 36.29 %.

Let us compare previous findings with the well-known digital measurement approach. If an A/D converter, with the same resolution (6 bits) and the input range (5 V) as in Table 1 is used, then its quantization step is:

$$q=2R/2^6=5V/64=78mV \qquad (6)$$

In Fig.7. this quantization step is compared with previously found DSM errors. It can be noticed that DSM

errors for the signals without discontinuities (50 Hz sine and triangle wave) are below the typical A/D quantization step. However, DSM errors are much above the typical A/D quantization step for the signals with significant discontinuities (40 Hz sine wave, 50 Hz square wave and 50 Hz sawtooth wave).

Of course, in the state of the art instruments based on the classical digital measurement approach, where A/D converters with very high resolution are used, quantization steps are drastically lower. For example, if 24-bit A/D converter is used, with the same input range, then its quantization step is:
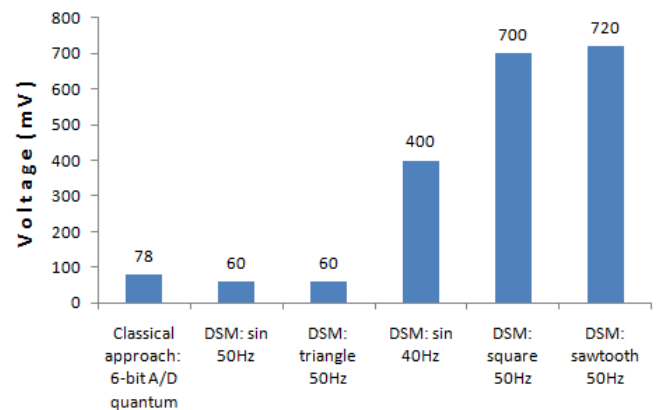
$$q=5V/2^{24}=0.29\mu V \qquad (7)$$

Fig.7. Comparison of DSM maximal errors with quantization step of 6-bit A/D conversion.

In the DSM approach, if there are no signal discontinuities, although measurement uncertainty can also be lowered by choosing an A/D converter with higher resolution, there are two other techniques of lowering measurement uncertainty [16-20, 25]:

- by increasing sampling rate;
- by extending measurement interval (this technique is limited only for periodic signals).

According to (5) measurement uncertainty is inversely proportional to $\sqrt{N}$, where N is the number of samples over a measurement interval. For example, if in measurement of 50 Hz sine wave we use 100 times faster A/D converter and have measurement interval of 2 seconds (100 periods included), we could expect error not greater than 60 mV/$\sqrt{100 \cdot 100}$ =0.6 mV. Notice that the EEG signal range after conditioning is amplified - e.g., if 10^4 amplification is applied, than the conditioned signal range is up to $10^4 \cdot 300$ μV=3 V.

From the perspective of comparing application of the DSM approach with application of the classical approach in EEG measurement, these results and analysis are not enough. However, these results certainly indicate the problem of the Wilbraham-Gibbs phenomenon when a signal with discontinuities is measured by the DSM approach. Discontinuities at the edges of measurement interval will certainly appear while measuring EEG signal by the DSM approach, though these discontinuities are not

expected to be as large as in previously measured waveforms. Therefore, the next section will directly investigate digital stochastic measurement of EEG signal in the time domain and compare it to the classical approach.

B. Measurement of EEG signal.

The source of the input signal in experimental measurements is not the human subject, but an artificial source – EEG signal generator, because repeatability of the input signal could not be achieved with a human subject and "live" measurement for each experiment. Of course, the input signal is not arbitrary formed, but generated from records previously measured by standard EEG measurement instrument.

This EEG signal generator is made by a development board with a programmable system-on-chip (PSoC) CY8C27843, using an embedded 8-bit digital-to-analog (D/A) converter, 16-bit counter and lookup table. Samples of the EEG signal, amplified 10^4 times, are stored in the lookup table, while the sampling rate is configured to be 3.840 Hz which provides relatively smooth analog signal at the output.

Parameters of the digital stochastic instrument are the same as in Table 1., except the number of measured Fourier coefficients – now DC component and 7 sine and 7 cosine Fourier coefficients are measured. Photo of the instrument is shown in Fig.8. and the block diagram of the instrument is shown in Fig.9. The multipliers and accumulators are implemented by the FPGA device (chip Cypress CY39100) which, by the help of microprocessor Atmel AT89S8252,

finally calculates Fourier coefficients. The microprocessor also interfaces the instrument with a PC. Pseudo-stochastic dither signal is generated by FPGA chip and analog adder is required for performing summation of the input signal and dither. The memory is flash EEPROM memory M29F040. A/D converter properties are the same as in simulations (resolution is m_1=6 bits, input range is ± 2.5 V, while the sampling rate is f_{ADC}=15625 Hz).

FPGA chip is programmed with a very-high-speed integrated circuits hardware description language (VHDL) program, and the VHDL program is comprised of 4 simultaneous processes (P1, P2, P3 and P4). The process P1 receives 6-bit digital values from A/D converter, while the process P2 is the main process by which all the mathematical calculations are implemented. The process P3 has the task to send the results of the process P2 to the microprocessor, while the process P4 waits for request from the microprocessor. When the request comes in, P4 activates the process P3. PC software application receives the data from the microprocessor, and performs recording and presenting of the measurement results.

A comparison of input signal and result of measurement, in this case, is presented in Fig.10. The maximal error is 6.14 μV, while the maximal error relative to the range of input signal is 18.32 %. As it was expected, according to the results with typical waveforms, the measurement error also increases at the edges of the measurement interval. Totally, 250 experimental measurements with 250 different EEG sequences of 20ms are performed, and the average maximal error relative to the range of input signal is 16.84 %.
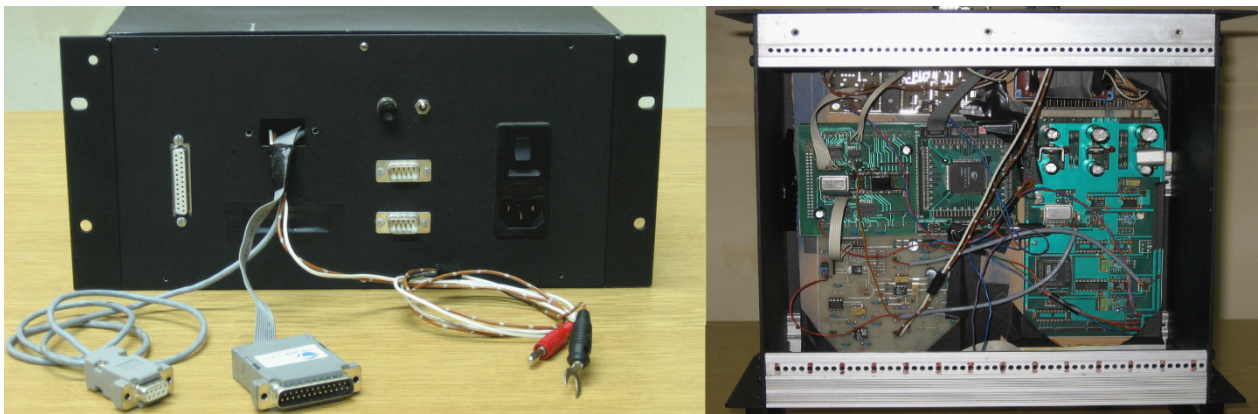

Fig.8. Digital stochastic instrument (connectivity panel at the left side of the figure, and interior PCBs at the right side).
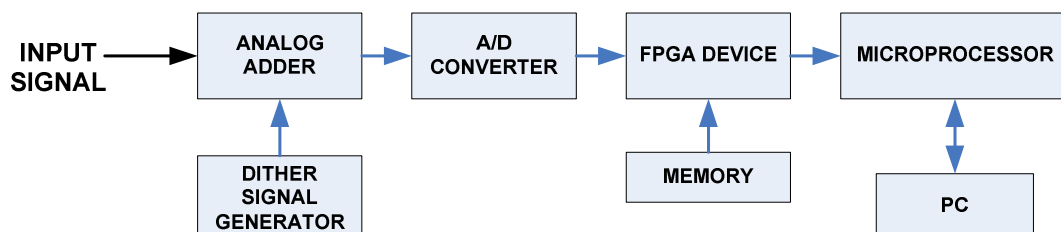

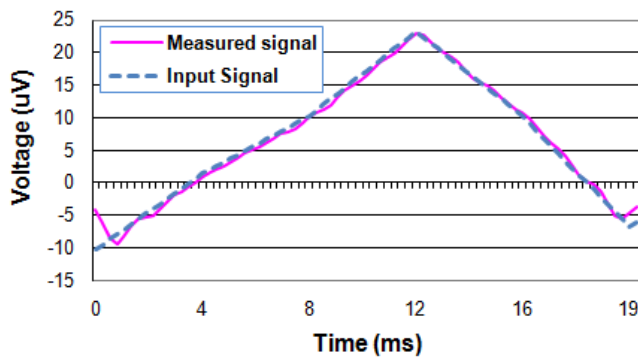Fig.9. Block diagram of digital stochastic instrument.

Fig.10. Result of measurement vs. input EEG signal for 20 ms measurement interval.

It is known that FFT of brain potential is usually calculated for a short section of time series - from 1 to 8 seconds [2]. Also, analyzing the results of EEG measurement with 20 ms interval, we assumed that for larger measurement intervals (e.g. 2 seconds), there would be no high discontinuities in the input signal, providing lower measurement errors due to the Wilbraham-Gibbs phenomenon. Having these in mind, the next simulation was performed with the properties presented in Table 2. 200 sine and cosine Fourier coefficients were measured, because fundamental frequency was 0.5 Hz and we wanted to cover the whole spectrum of the EEG signal (up to 100 Hz). Input signal was also generated from EEG records previously measured by the standard EEG measurement instrument.

Table 2. Properties of measurement system with 2s measurement interval.

Property	Values
A/D conversion (Fig. 3)	Resolution: m_1=6 bits Input range: ±R and R=2.5 V Sampling frequency: f_{ADC} = 1000 Hz
Dither d_1	$0 \le |d_i| \le 39.7 mV$
Measurement subinterval	[0,T] and T = 2 s
Fundamental frequency	f_0 = 1/T = 0.5 Hz
Number of samples per measurement subinterval	N = 2000
Digital dithered base functions	Stored in memory in 64-bit floating point resolution but passed to the multiplier in 8-bit resolution, thus faithfully simulating an A/D converter with properties: Resolution: m_2 = 8 bits Range: ±R and R=2.5 V Sampling frequency: f_{ADC} = 1000 Hz
Number of measured Fourier coefficients	DC component + 200 sine coefficients + 200 cosine coefficients

A comparison of input signal and result of this measurement is presented in Fig.11. The maximal error is 0.96 µV, while the maximal error relative to the range of input signal is 1.44 %. In total, 250 measurements were simulated with 250 different EEG sequences of 2 s, resulting in average maximal relative error of 1.37 %.

The results show that digital stochastic measurements of EEG signal in the time domain are less affected with the Wilbraham-Gibbs phenomenon when measurement interval is 2 s, in comparison to the system when measurement interval is 50 ms. Respectively, digital stochastic measurement of EEG signal in the time domain is more accurate for 2 s measurement interval, than for 50 ms measurement interval.

It is interesting to compare these results with metrological characteristics for electroencephalographs [31] recommended by Organisation Internationale de Métrologie Légale (OIML), but also with classical digital measurement approach. The dynamic value of relative voltage measurement error, dependent on sensitivity-setting and input voltage range, is required in [31]. It can be easily determined that, for the lowest sensitivity-setting (1 µV/mm) and the lowest input voltage range (5 µm) of the EEG instrument, the absolute error limit is 1 µV.
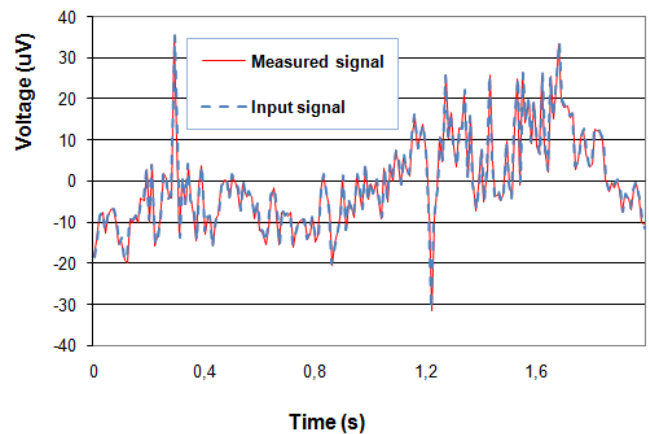

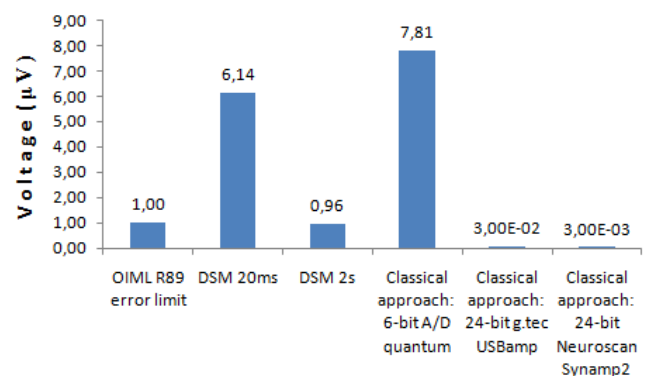Fig.11. Result of measurement vs. input EEG signal for 20ms measurement interval.

Fig.12. Comparison of DSM maximal errors with the error limit required in [31] (OIML R89 error limit) and A/D quantization steps.

Comparison of DSM maximal errors with the error limit required in [31] and A/D quantization steps is presented in Fig.12. For classical approach, 6-bit A/D converter, 24-bit EEG instrument *g.tec USBamp* [32] and 24-bit *Neuroscan Synamp2* [33] are included. It can be noticed that the DSM maximal error for 2 s measurement interval is below the limit in [31]. Also, this error is lower than the 6-bit quantization step, but much higher than the quantization step of 24-bit instruments.

If we disregard influence of the instrument intrinsic noise and ambient noise, and if the goal is to design an EEG instrument with the measurement error much below the limit in [31], then advantage of classical approach with 24-bit A/D converter is obvious. If the goal is to design an instrument with sufficient accuracy (error below the limit in [31]), then the DSM approach can be utilized. Benefit of implementing the DSM approach is its simple hardware design, based on a simple flash A/D converter. Relatively low sampling rate (1 kHz) is used in the proposed DSM instrument. However, if the sampling rate is increased, then, according to (5), measurement uncertainty will not be higher even if the flash A/D converter with a lower resolution (e.g., 4 bits) is used. Utilization of such low-resolution and fast flash A/D converter would provide even simpler hardware design, enabling integration of the DSM module into simple low-power integrated circuit.

If we include the influence of the instrument intrinsic noise and ambient noise, we can notice that noise voltage can be much above the quantization step of typical EEG devices - especially of advanced ones. For example, it is claimed for Neuroscan Synamp2 [33], which uses 24-bit A/D converter, that the intrinsic noise is less than 0.4 μV (this limit is 133 times greater than its quantization step). This noise is superimposed on measurement result as it is (without any attenuation), while in digital stochastic instruments the noise is highly attenuated [18, 25] regardless of its origin – whether the noise is the device intrinsic noise or ambient noise interfered at the device input. From this perspective, it can be noticed that another benefit of the DSM approach is its high robustness to the noise.

4. CONCLUSION

Digital stochastic measurement of EEG signal harmonics was introduced in the past. This paper investigates digital stochastic measurement of EEG signal in the time domain, emphasizing the problem of the influence of the Wilbraham-Gibbs phenomenon on measurement accuracy. The increase of measurement error, related to the Wilbraham-Gibbs phenomenon, is found and analyzed for some typical forms of stationary signals and for the EEG signal. While measuring the EEG signal, the measurement error is lowered when measurement interval is extended from 50 milliseconds to 2 seconds; more precisely, the average maximal error relative to the range of input signal is decreased from 16.84 % to 1.37 %. According to those findings, our proposition, for designers of EEG instruments based on the DSM approach, is to design the instrument with 2 seconds measurement interval.

The DSM maximal errors are compared with the error limit being required in [31] and the quantization steps of 6-bit and 24-bit devices, based on well-known digital measurement approach. It can be noticed that the DSM maximal error for 2 s measurement interval is below the limit in [31], lower than the 6-bit quantization step, but much higher than the 24-bit quantization steps.

If we disregard influence of the instrument intrinsic noise and ambient noise, and if the design goal is an EEG instrument with the measurement error much below the limit in [31], then the advantage of classical approach with 24-bit A/D converter is obvious and the DSM approach could not enable the required accuracy. If the design goal is an instrument with sufficient accuracy (i.e., the error below the limit in [31]), then the DSM approach can be used, benefiting from the hardware simplicity of the method.

If we include the noise influence, it can be noticed that noise voltage can be much above the quantization step in EEG devices, based on classical digital measurement approach. As the noise is highly attenuated in digital stochastic instruments, high robustness to the noise can be another reason for choosing the DSM based design.

REFERENCES

[1] Teplan, M. (2002). Fundamentals of EEG measurement. *Measurement Science Review*, 2 (2), 1-11.

[2] Bronzino, J.D. (2000). Principles of electroencephalography. In Bronzino, J.D. (ed.) *Biomedical Engineering Handbook*, (2nd ed.). CRC Press, 1-13.

[3] Webster, J.G. (1998). *Medical Instrumentation Application and Design* (11th ed.). Wiley.

[4] Abeles, M., Goldstein, M. (1977). Multispike train analysis. *Proceedings of the IEEE*, 65 (5), 762-773.

[5] Winter, B.B., Webster, J.G. (1983). Driven-right-leg circuit design. *IEEE Transactions on Biomedical Engineering*, 30 (1), 62-66.

[6] Kutz, M. (2003). *Standard Handbook of Biomedical Engineering and Design*. McGraw-Hill.

[7] Schnitz, B.A., Stewart, J.A., Allen, R.V., Fadem, K.C. (2004). *Improving signal quality and test reliability in EEG measurements using integrated high-density surface-mount electronics*. http://ebook.lib.sjtu.edu.cn/smat/Files/S2-3.pdf.

[8] Teplan, M., Krakovská, A., Štolc, S. (2003). EEG in the context of audiovisual stimulation. *Measurement Science Review*, 3 (2), 17-20.

[9] Teplan, M., Krakovská, A., Štolc, S. (2006). Short-term effects of audio-visual stimulation on EEG. *Measurement Science Review*, 6 (4), 67-70.

[10] Krakovská, A., Štolc, S. (2006). Fractal complexity of EEG signal. *Measurement Science Review*, 6 (4), 63-66.

[11] Šušmáková, K., Krakovská, A. (2007). Classification of waking, sleep onset and deep sleep by single measures. *Measurement Science Review*, 7 (4), 34-38.

[12] Šušmáková, K. (2006). Correlation dimension versus fractal exponent during sleep onset. *Measurement Science Review*, 6 (4), 58-62.

[13] von Neumann, J. (1956). Probabilistic logic and the synthesis of reliable organisms from unreliable components. In Shannon, C., McCarthy, J. (eds.) *Automata Studies*. Princeton University Press, 43-98.

[14] Wagdy, M.F., Ng, W. (1989). Validity of uniform quantization error model for sinusoidal signals without and with dither. *IEEE Transactions on Instrumentation and Measurement*, 38 (3), 718-722.

[15] Kamenský, M., Kováč, K. (2011). Correction of ADC errors by additive iterative method with dithering. *Measurement Science Review*, 11 (1), 15-18.

[16] Vujičić, V., Milovančev, S., Pešaljević, M., Pejić, D., Župunski, I. (1999). Low frequency stochastic true RMS instrument. *IEEE Transactions on Instrumentation and Measurement*, 48 (2), 467-470.

[17] Pejic, D., Vujicic, V. (2000). Accuracy limit of high-precision stochastic Watt-hour meter. *IEEE Transactions on Instrumentation and Measurement*, 49 (3), 617-620.

[18] Santrač, B., Sokola, M.A., Mitrović, Z., Župunski, I., Vujičić, V. (2009). A novel method for stochastic measurement of harmonics at low signal-to-noise ratio. *IEEE Transactions on Instrumentation and Measurement*, 58 (10), 3434-3441.

[19] Pjevalica, V., Vujičić, V. (2010). Further generalization of the low-frequency true-RMS instrument. *IEEE Transactions on Instrumentation and Measurement*, 59 (3), 736-744.

[20] Antić, B.M, Mitrović, Z.L, Vujičić V.V. (2012). A method for harmonic measurement of real power grid signals with frequency drift using instruments with internally generated reference frequency. *Measurement Science Review*, 12 (6), 277-285.

[21] Angeloneb, L.M., Purdona, P.L., Ahveninena, J., Belliveaua, J.W., Bonmassara, G. (2006). EEG/(f)MRI measurements at 7 Tesla using a new EEG cap ("InkCap"). *NeuroImage*, 33 (4), 1082-1092.

[22] Negishi, M., Pinus, B.I., Pinus, A.B., Constable, R.T. (2007). Origin of the radio frequency pulse artifact in simultaneous EEG-fMRI recording: Rectification at the carbon-metal interface. *IEEE Transactions on Biomedical Engineering*, 54 (9), 1725-1727.

[23] Mirsattari, S.M., Ives, J.R., Leung, S., Menon, R.S. (2007). EEG monitoring during functional MRI in animal models. *Epilepsia*, 48 (4), 37-46.

[24] Allen, P.J., Josephs, O., Turner, R. (2000). A method for removing imaging artifact from continuous EEG recorded during functional MRI. *NeuroImage*, 12 (2), 230-239.

[25] Sovilj, P.M., Milovančev, S.S., Vujičić, V. (2011). Digital stochastic measurement of a nonstationary signal with an example of EEG signal measurement. *IEEE Transactions on Instrumentation and Measurement*, 60 (9), 3230-3232.

[26] Sovilj, P., Vujičić, V., Pjevalica, N., Pejić, D., Urekar, M., Župunski, I. (2013). Influence of signal stationarity on digital stochastic measurement implementation. *Electronics*, 17 (1), 45-53.

[27] Wilbraham, H. (1848). On a certain periodic function. *The Cambridge and Dublin Mathematical Journal*, 3, 198-201.

[28] Gibbs, J.W. (1899). Fourier's series. *Nature*, 59 (1539), 606.

[29] Hazewinkel, M. (2001). Gibbs phenomenon. In *Encyclopedia of Mathematics*. Springer.

[30] Smith, S.W. (1999). *The Scientist and Engineer's Guide to Digital Signal Processing* (2nd ed.). California Technical Publishing, 141-168.

[31] International Organization of Legal Metrology. (1990). *Electroencephalographs - Metrological characteristics - Methods and equipment for verification*. OIML R 89, Edition 1990 (E).

[32] g.tec – Guger Technologies, http://www.gtec.at.

[33] Compumedics Neuroscan, http://compumedicsneuro scan.com/products-overview/.